THE ASTROPHYSICAL JOURNAL, 445:L91–L94, 1995 June 1

DETERMINING THE MOTION OF THE LOCAL GROUP USING TYPE Ia SUPERNOVAE LIGHT CURVE SHAPES

ADAM G. RIESS, WILLIAM H. PRESS, AND ROBERT P. KIRSHNER
Harvard-Smithsonian Center for Astrophysics, 60 Garden Street, Cambridge, MA 02138
Received 1994 December 5; accepted 1995 March 20

ABSTRACT

We have measured our Galaxy's motion relative to distant galaxies in which Type Ia supernovae (SNe Ia) have been observed. The effective recession velocity of this sample is 7000 km s^{-1}, which approaches the depth of the survey of brightest cluster galaxies by Lauer & Postman (1994). We use the light curve shape (LCS) method for deriving distances to SNe Ia, providing relative distance estimates to individual supernovae with a precision of $\sim 5\%$ (Riess, Press, & Kirshner 1995). Analyzing the distribution on the sky of velocity residuals from a pure Hubble flow for 13 recent SNe Ia drawn primarily from the Calán/Tololo survey (Hamuy 1993a, 1994, 1995a, b; Maza et al. 1994), we find the best solution for the motion of the Local Group in this frame is 600 ± 350 km s^{-1} in the direction $l = 260°$, $b = +54°$, with a 1 σ error ellipse that measures $90° \times 25°$. This solution is consistent with the rest frame of the cosmic microwave background (CMB) as determined by the *COBE* measurement of the dipole temperature anisotropy, and also with many plausible bulk flows expected to accompany observed density variations. It is inconsistent with the velocity observed by Lauer & Postman.

Subject headings: cosmology: observations — large-scale structure of universe — Local Group — supernovae: general

1. INTRODUCTION

The motions of galaxies provide a dynamical measure of the way mass and light are distributed in the universe. Rubin et al. (1976) and Rubin (1977) used giant Sc spiral galaxies as distance indicators to find evidence for a 600 km s^{-1} coherent motion of neighboring galaxies out to 3500–6500 km s^{-1}. Many subsequent attempts to measure motion that departs from smooth expansion combine redshifts with distance measures (Burstein 1990; Strauss & Willick 1995). This approach yields detections of local flows attributed to nearby mass concentrations (Virgo, Hydra-Centaurus, Great Attractor) of substantial scale and amplitude. Recently, Lauer & Postman (1994, hereafter LP) surveyed the brightest cluster galaxies from Abell clusters and inferred that, remarkably, a volume of space out to 8000–11,000 km s^{-1} is moving at 560 km s^{-1} with respect to the CMB frame. This lack of convergence to the CMB frame is hard to understand in conventional pictures of structure formation (Strauss et al. 1995) and invites investigation by independent methods. This measurement requires a bright distance indicator that is useful out to 10,000 km s^{-1} and which is precise enough to detect velocity residuals of order 600 km s^{-1}.

The narrow luminosity distribution of Type Ia supernovae (SNe Ia) suggests that they can provide deep and accurate distance estimates, and information in the light curve shape has improved the usefulness of these objects for cosmological measurements (Phillips 1993; Hamuy et al. 1995a). We have developed statistical tools to derive distances using distance independent information contained in supernova light curves (Riess, Press, & Kirshner 1995, hereafter RPK). Following Phillips (1993), the method relies on a "training set" of light curves for supernovae in galaxies with accurate relative distance measurements. This determines the correlation between luminosity and light curve shape. When applied to an independent set of 13 distant SNe Ia light curves drawn primarily from the Calán/Tololo survey (Hamuy et al. 1993a, 1994, 1995a, b; Maza et al. 1994; Ford et al. 1993; Riess et al. 1995), the light curve shape (LCS) method provides more precise distance estimates than the standard candle assumption, reducing the dispersion around a Hubble line from 0.5 to 0.18 mag. The LCS method also predicts individual distance uncertainties as listed in Table 1: the median LCS distance error for our 13 supernovae is 5%, with the rest of the dispersion accounted for by random and bulk flow velocities. Although our sample is small, the LCS distances are precise enough to provide information about the velocity residuals from a pure Hubble flow.

2. MEASURING THE LOCAL GROUP MOTION WITH TYPE Ia SUPERNOVAE

We fit a Hubble line to 13 supernovae (analyzed using LCS; see Table 1) to determine simultaneously H_0 (which we have discussed elsewhere; see RPK) and three Cartesian velocity components of the mean rest frame of the host galaxies with respect to the Local Group. Transformation from heliocentric redshifts to the Local Group rest frame is done by addition of the vector $(-30, 297, -27)$ km s^{-1} in Galactic Cartesian coordinates (de Vaucouleurs et al. 1991; Lynden-Bell & Lahav 1988).

For comparing dipole hypotheses, we use a χ^2 statistic:

$$\chi^2(H_0, \boldsymbol{v}_{\rm LG}) = \sum_{i=1}^{13} \frac{[cz_i - H_0 10^{0.2(\mu_i - 25)} + \boldsymbol{v}_{\rm LG} \cdot \hat{\boldsymbol{r}}_i]^2}{\sigma_i^2}, \quad (1)$$

where $\boldsymbol{v}_{\rm LG}$ is the Local Group velocity vector, μ_i is the LCS distance modulus of the ith supernova, z_i is its redshift, $\hat{\boldsymbol{r}}_i$ is the unit vector in the direction of the supernova, H_0 is the Hubble constant in km s^{-1} Mpc^{-1}, and σ_i^2 is the quadrature sum of all distance and velocity errors. Our distance uncertainties from the LCS method are based on our ability to reconstruct the light curve observations (RPK). Another source of distance error which we explore in § 4 is host galaxy absorption. In addition, individual supernovae have motions that are not completely modeled by a pure Hubble flow plus a motion of

TABLE 1

SNe Ia PARAMETERS

SN	log v (km s^{-1})	l	b	μ(LCS)[a]	$\sigma_{\mu(LCS)}$
1992bo.....	3.753	261°.88	−80°.35	34.53	0.09
1992bc.....	3.782	245.70	−59.64	34.48	0.08
1992K	3.451	306.28	16.31	33.15	0.38
1992aq.....	4.485	1.78	−65.32	38.21	0.08
1992ae.....	4.350	332.7	−41.99	37.68	0.09
1992P.....	3.872	295.62	73.11	35.39	0.06
1992J	4.120	263.55	23.54	36.88	0.13
1991U	3.968	311.82	36.21	36.02	0.13
1991ag.....	3.618	342.56	−31.64	33.90	0.06
1990af	4.178	330.82	−42.24	36.62	0.07
1992G	3.257	184.62	59.84	32.57	0.08
1991M.....	3.396	30.39	45.90	33.11	0.17
1993ae.....	3.769	144.62	−63.23	34.54	0.14

[a] μ is our distance modulus; $\sigma_{\mu(LCS)}$ is the statistical uncertainty from LCS; log v values from Cerro Tololo Inter-American Observatory.

the Local Group. Random velocities (RVs) of galaxies are clearly evident in the velocity residuals of our sample. We find that adopting RV anywhere in the range of 275–800 km s^{-1} yields the expected range of χ^2 for 9 degrees of freedom (13 less 3 velocity components and H_0), with little sensitivity to the value of RV. We adopt RV = 470 km s^{-1}, which yields a χ^2 per degree of freedom of 1 and is consistent with 400 ± 139 km s^{-1}, derived from the recent pairwise difference estimate from the CFA redshift survey (Marzke et al. 1995).

Minimizing χ^2 with respect to the four free parameters determines the best values; the error for each dipole component is its 68% confidence limit considered separately (i.e., when χ^2 is minimized with respect to the other components): $H_0 = 66$ km s^{-1} Mpc^{-1}, $V_x = -90 \pm 370$ km s^{-1}, $V_y = -510 \pm 510$ km s^{-1}, and $V_z = 710 \pm 220$ km s^{-1}. Our calibration of the SNe Ia peak magnitude, derived from the *Hubble Space Telescope* (*HST*) Cepheid distance to SN 1972E (RPK; Sandage et al. 1994), affects only our estimate of H_0 and not these velocity components. The weighted mean recession velocity of our sample is 7000 km s^{-1}. To visualize the dipole present in our sample, Figure 1 plots the residual recession velocity from the best Hubble fit (in the velocity rest frame of the Local Group, i.e., $v_{LG} = 0$) versus the location on the sky for each supernova. The systematic pattern of residuals which is evident in this figure clearly shows our motion with respect to these galaxies.

Joint confidence regions for the four fitted parameters at various confidence levels can be determined in the standard way (Avni 1976; Press et al. 1992), as ellipsoids whose boundaries correspond to specified values for $\Delta\chi^2$. In this case, we determine joint confidence regions for the three velocity parameters V_x, V_y, and V_z, with the fourth parameter (H_0) chosen to minimize χ^2 for each value of (V_x, V_y, V_z). With 3 degrees of freedom in the resulting joint confidence region, the boundary of the 68% confidence region lies at $\Delta\chi^2 = 3.5$, the boundary of the 95% confidence region lies at $\Delta\chi^2 = 8.0$, and the boundary of the 99% confidence region lies at $\Delta\chi^2 = 11.3$.

We can now ask where the *COBE* rest frame, and the LP rest frame, lie with respect to these confidence regions: when the *COBE* frame (10, −542, 300) km s^{-1} is used, $\chi^2 = 12.5$ (DOF = 9) and $\Delta\chi^2 = 3.5$. This is inside the 68% confidence region: our measurement of the Local Group motion is consistent with the *COBE* dipole. For the LP frame (−470, −399, −333) km s^{-1}, $\chi^2 = 32.7$ (DOF = 9), so $\Delta\chi^2 = 23.7$. This lies outside the 99% confidence region. In fact, it is ruled out at greater than the 99.99% ("greater than 3 σ") confidence level. We can also determine our consistency with the LP measurement as well as the specific LP rest frame by adding our errors in quadrature with theirs and evaluating the confidence level with which we can say the difference between the two measurements is zero. Including the errors of both measurements yields a reduced rejection level of 99.45%. Alternatively, we find that the most likely dipole vector for our measurement and the LP measurement taken jointly is (−340, −420, 140), but with a

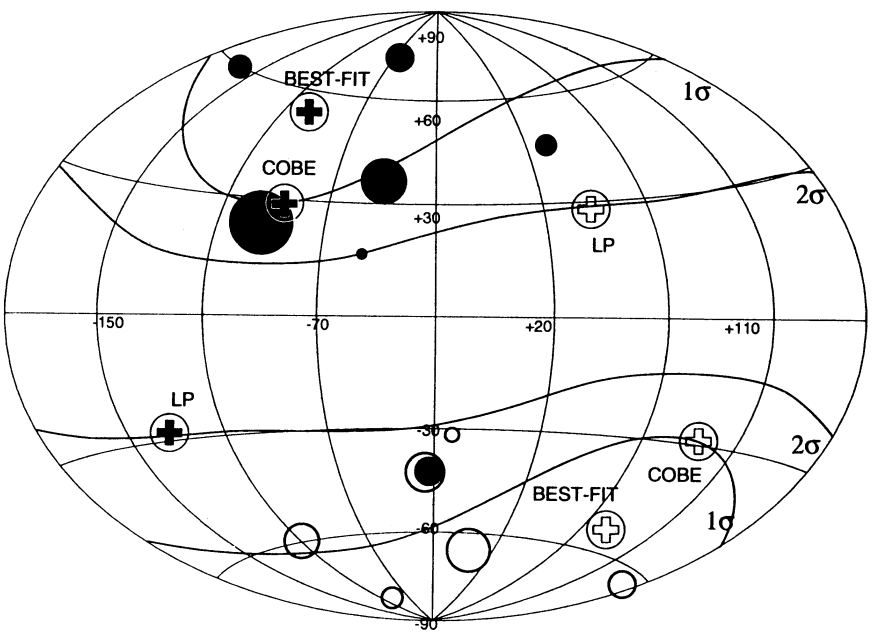

FIG. 1.—Hubble diagram velocity residuals and predicted Local Group motion on the sky. Filled/open points represent supernovae with negative/positive residual velocity; the areas of the points correspond to the magnitude of the velocity residual. Filled/open crosses show the direction toward which the Local Group is approaching/receding according to the best fit for the data in this Letter, the *COBE* satellite, and Lauer & Postman's survey of brightest cluster galaxies. Contours of 1 and 2 σ are displayed for the direction of the best fit to the supernova residual velocities. Coordinates are galactic, with the central meridian at 335°.

joint likelihood of 0.7% or a mutual rejection of 99.3%. We have also compared our measurement with the *IRAS* dipole, deduced by peculiar accelerations, and found a high level of consistency ($\Delta\chi^2 = 1.2$; Rowan-Robinson et al. 1990). Finally, we can reject the null hypothesis, i.e., no net motion of the Local Group with respect to the supernova frame, at the 99% confidence level.

Our ability to exclude the LP rest frame at interesting confidence levels derives from the small dispersion of the LCS method, yet the same trend is present at lower precision if the analysis is redone assuming SNe Ia to be identical standard candles with 20% distance uncertainty. The relevant χ^2 values are 13.5 (best-fit), 14.5 (*COBE*), 16.4 (no net motion), and 21.7 (LP). The standard-candle frame would be consistent with *COBE* or zero motion, and inconsistent with LP, but naturally with a lower certainty when using the poorer standard-candle assumption. That is because there are real variations in the supernova luminosities which are successfully accounted for by LCS. Previous attempts to use SNe Ia as standard candles to measure motions of the Local Group have probably suffered from poor photographic data and contained samples which were too nearby to avoid local flows (Jerjen & Tammann 1993; Miller & Branch 1992).

3. SAMPLE BIAS AND ROBUSTNESS

Because supernovae are discovered at high Galactic latitude, our measurement of the motion is better in the z-direction which points out of the Galactic plane than in the x- and y-directions along the Galactic plane. The LP frame predicts motion in the z-direction with the opposite sign at $V_z = -333$ km s^{-1}, and this difference accounts for our strong statistical rejection of that motion. We note that the maximum likelihood scalar length of our dipole, 600 km s^{-1}, is smaller than the 880 km s^{-1} which one would naively derive from the Cartesian components (biased to higher values by the uncertainties; see Kendall & Stuart 1976, p. 97).

We considered the effects of sparse sampling and clustering on our ability to resolve a dipole. Measurement of a dipole in a complex velocity field from a limited number of objects can be distorted by small-scale velocity patterns (Kaiser 1988; Feldman & Watkins 1994). Uroš Seljak (private communication) has calculated the window function for our sample and convolved it with a standard cold dark matter (CDM) power spectrum to determine the components of the covariance matrix and thus estimate the dipole components and their uncertainty. This procedure yields a maximum likelihood estimate of $(-42 \pm 445, -517 \pm 575, 716 \pm 276)$ km s^{-1} which is highly consistent with the value and uncertainty we derive for the dipole without considering these effects. Including velocity correlations also yields a greater consistency with the *COBE* dipole ($\Delta\chi^2 = 2.4$) and a reduced lower bound on the rejection of the LP frame (99.8%) and the LP measurement (98.4%). The latter is a lower bound because the two samples measure some of the same space (e.g., SN 1993ae is in Abell 194) and have some small-scale flows in common. We intend to pursue N-body simulations to see how SNe Ia can be used to discriminate among cosmological models (Seljak et al. 1995).

We also performed a series of jackknife tests to assess the influence of outliers on our results, with the conclusion that our results are robust against deleting any one or two supernovae from the sample. For example, removing the two farthest supernovae (new effective velocity = 5900 km s^{-1}), the two nearest supernovae (new effective velocity = 8200 km s^{-1}) or the two supernovae with largest distance uncertainty had no significant effect on any of the results.

To evaluate the reliability of our uncertainty estimates, we performed a Monte Carlo simulation with 100,000 synthetic data sets of 13 supernovae with the same positions and uncertainties as ours, as displayed in Figure 2. These simulations verify our $\Delta\chi^2$ uncertainty estimates to within 1% and demonstrate our ability to discriminate systematic motions on the basis of 13 accurate distance indicators of wide spatial distribution. Our most likely agreement with *COBE* is at the 1 σ level; the most likely rejection of the LP frame is at 3 σ level. In recovering our dipole, we find a small geometric bias (of 9, -28, -3) km s^{-1} incurred by simultaneously solving for the expansion and the motion of a sample which is not uniformly distributed over the sky.

Finally, in an effort to test the validity of our results free from the choice of an error model, we performed a bootstrap resampling test. This test uses only the values of the data to measure the uncertainty of the dipole parameters solely from the distribution of the data points around their expectation without using any weighting scheme. This test confirms the implication of our error model; there is little room in the dispersion for other sources of error, and it shows that any unmodeled sources remaining do not affect our primary

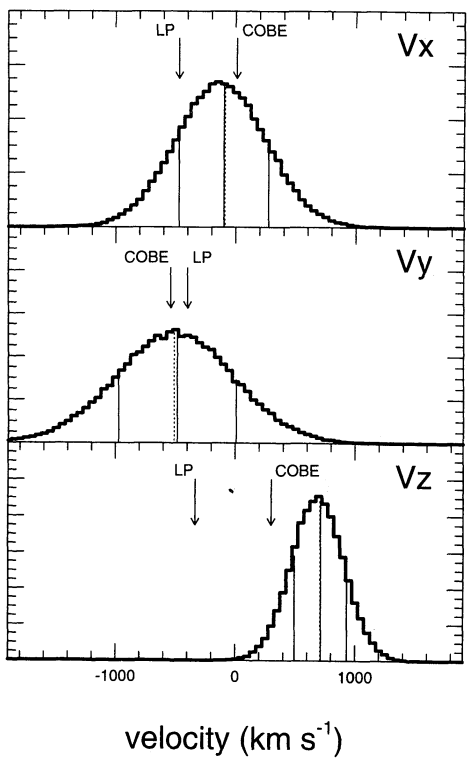

FIG. 2.—Monte Carlo dipole recovery simulation. A total of 100,000 synthetic data sets of 13 supernovae were created with the same positions and uncertainties as our sample and our adopted dipole motion of (-90, -150, 710) km s^{-1}. These are the distributions of the Cartesian components of the dipole recovered from each synthetic data set. The difference between the mean (*solid line*) and the adopted dipole (*dotted line*) represents a geometric bias of (9, -28, -3) km s^{-1} The 1 σ boundaries (*outer solid lines*) confirm the χ^2 errors to within 1%. The arrows show the *COBE* and LP measurement of the dipole components. This simulation also verified our most likely agreement with *COBE* to be at the 1 σ level and the most likely disagreement with LP to be at the 3 σ level. The difference between our result and the LP result is most conspicuous in the z-direction.

results: in this case, an agreement with *COBE* at the 1 σ level and a 99% rejection of the LP measurement.

4. EFFECT OF ABSORPTION

Although the Hubble fit residuals, supernova spectra, and resampling test suggest that there is little host galaxy absorption present in our sample, we investigated how absorption could affect our conclusions. Our corrections for galactic absorption (Burstein & Heiles 1982) are small, and omitting these corrections does not alter our result. Host absorption appears to be small in our sample. None of the supernova spectra showed strong Na I D absorption (Hamuy et al. 1995b). Using color information within the LCS framework may provide useful estimates of absorption for individual objects and increase the precision of distance estimates.

A constant absorption different from zero would affect our estimate of H_0, but not our measurement of the dipole. The presence of significant host absorption for only a few objects would be detected by the jackknife test: as we discovered in § 3, removing any one or two objects had little effect on our conclusions. Only a scatter about the mean host absorption could affect our dipole measurement.

We considered the largest allowed estimate of error from host absorption that is still consistent with the observed residuals from the Hubble line. This error model consisted of adopting Marzke's value RV = 400 km s^{-1} and then adding in quadrature the largest scatter around the mean absorption which still maintains a significant χ^2, $\chi^2 = N - (2N)^{1/2}$ where N is the degrees of freedom. This intentional inflation of our overall error accommodates up to 0.15 mag of scatter around the mean host absorption and gives the best dipole measurement as $(0 \pm 390, -310 \pm 550, 620 \pm 250)$ km s^{-1}. For this error model, the *COBE* frame is within the 45% confidence level; we reject the no net motion hypothesis at the 90% level, we disagree with the LP frame at the 99.9% confidence level, and we disagree with the LP measurement at the 98% confidence level. For this sample it makes little difference which error model we choose. In future work, we intend to use the LCS technique in more than one color to make individual estimates of total absorption.

5. INTERPRETATION

Our result is consistent with the *COBE* rest frame and some moderate bulk flows but not with that proposed by LP. Although our effective velocity is 7000 km s^{-1} and the Abell Cluster inertial frame used by LP is effectively in the range of 8000–11,000 km s^{-1}, we can easily extend our result up to 8000 km s^{-1} by excluding two nearby supernovae. In addition, LP have reduced the effective velocity of their sample to 5000 km s^{-1} by excluding distant clusters. Neither change affects the two derived motions or brings them into agreement.

The velocity difference between the supernova frame and the CMB frame at 7000 km s^{-1} is consistent with the difference expected from observed density fluctuations and the flows of order 200–400 km s^{-1} they would induce on these scales (A. Dekel, private communication). If both the supernova and the LP measurements were correct, this might indicate a nonuniformity of the galactic luminosity function on large scales. With an enlarged supernova sample, we will attempt to confirm and further constrain these results.

David Spergel audaciously suggested that our small sample might constrain the large-scale flow. Tod Lauer, Marc Postman, Brian Schmidt, George Rybicki, and Jeff Willick contributed valuable discussions. We are grateful to Mario Hamuy, Mark Phillips, Nick Suntzeff, Bob Schommer, Josè Maza, and the entire Calán/Tololo collaboration for the opportunity to study their outstanding data. We also thank Uroš Seljak for providing large-scale structure calculations. This work was supported through grants AST 92-18475 and PHY 91-06678.

REFERENCES

Avni, Y. 1976, ApJ, 210, 642
Burstein, D. 1990, Rep. Prog. Phys., 53, 241
Burstein, D., & Heiles, C. 1982, AJ, 87, 1165
de Vaucouleurs, G., et al. 1991, in Third Reference Catalogue of Bright Galaxies (New York: Springer-Verlag)
Feldman, H. A., & Watkins, R. 1994, ApJ, 430, L17
Ford, C., et al. 1993, AJ, 106, 3
Hamuy, M., Phillips, M. M., Maza, J., Suntzeff, N. B., Schommer, R. A., & Avilés, A. 1994, AJ, 108, 6
———. 1995a, AJ, 109, 1
———. 1995b, in preparation
Hamuy, M., et al. 1993a, AJ, 106, 2392
Jerjen, H., & Tammann, G. A. 1993, A&A, 376, 1
Kaiser, N. 1988, MNRAS, 231, 149
Kendall, M., & Stuart, A., 1976, The Advanced Theory of Statistics, Vol. III (London: C. Griffin)
Lauer, T. R., & Postman, M. 1994, ApJ, 425, 418 (LP)
Lynden-Bell, D., & Lahav, O. 1988, in Large-Scale Motions in the Universe, ed. V. C. Rubin & G. V. Coyle (Princeton: Princeton Univ. Press), 199
Marzke, R. O., Geller, M. J., daCosta, L. N., & Huchra, J. P. 1995, AJ, submitted
Maza, J., Hamuy, M., Phillips, M., Suntzeff, N., & Avilés, R. 1994, ApJ, 424, L107
Miller, D. L., & Branch, D. 1992, AJ, 103, 379
Phillips, M. 1993, ApJ, 413, L105
Press, W. H., Teukolsky, S. A., Vetterling, W. T., & Flannery, B. P. 1992, Numerical Recipes (2d ed.; Cambridge: Cambridge Univ Press)
Riess, A. G., Press, W. H., & Kirshner, R. P. 1995, ApJ, L17, 438 (RPK)
Riess, A. G., et al. 1995, in preparation
Rowan-Robinson, M., et al. 1990, MNRAS, 247, 1
Rubin, V. C. 1977, ApJ, 211, L1
Rubin, V. C., Thonnard, N., Ford, W. C., & Roberts, M. S. 1976, AJ, 81, 687
Sandage, A., et al. 1994, ApJ, 423, L13
Seljak, U., et al. 1995, in preparation
Strauss, M. A., Cen, R., Ostriker, J. P., Lauer, T. R., & Postman, M. 1995, ApJ, 444, 507
Strauss, M. A., & Willick, J. A., 1995, Phys. Rep., in press